Neuropsychopharmacology (2011) 36, 519–528

www.neuropsychopharmacology.org

NMDA Receptor Hypofunction Phase Couples Independent γ-Oscillations in the Rat Visual Cortex

Himashi Anver[1], Peter D Ward[1], Andor Magony[1] and Martin Vreugdenhil*[,1]

[1]*Neuronal Networks Group, School of Clinical and Experimental Medicine, University of Birmingham, Birmingham, United Kingdom*

Hallucinations, a hallmark of psychosis, can be induced by the psychotomimetic *N*-methyl-D-aspartic acid (NMDA) receptor antagonists, ketamine and phencyclidine (PCP), and are associated with hypersynchronization in the γ-frequency band, but it is unknown how reduced interneuron activation associated with NMDA receptor hypofunction can cause hypersynchronization or distorted perception. Low-frequency γ-oscillations (LFγ) and high-frequency γ-oscillations (HFγ) serve different aspects of perception. In this study, we test whether ketamine and PCP affect the interactions between HFγ and LFγ in the rat visual cortex *in vitro*. In slices of the rat visual cortex, kainate and carbachol induced LFγ ($\sim$34 Hz at 32°C) in layer V and HFγ ($\sim$54 Hz) in layer III of the same cortical column. In controls, HFγ and LFγ were independent, and pyramidal neurons recorded in layer III were entrained by HFγ, but not by LFγ. Sub-anesthetic concentrations of ketamine selectively decelerated HFγ by 22 Hz ($EC_{50} = 2.7\,\mu M$), to match the frequency of LFγ in layer V. This caused phase coupling of the two γ-oscillations, increased spatial coherence in layer III, and entrained the firing of layer III pyramidal neurons by LFγ in layer V. PCP similarly decelerated HFγ by 22 Hz ($EC_{50} = 0.16\,\mu M$), causing cross-layer phase coupling of γ-oscillations. Selective NMDA receptor antagonism, selective NR2B subunit-containing receptor antagonism, and reduced *D*-serine levels caused a similar selective deceleration of HFγ, whereas increasing NMDA receptor activation through exogenous NMDA, *D*-serine, or mGluR group I agonism selectively accelerated HFγ. The NMDA receptor hypofunction-induced phase coupling of the normally independent γ-generating networks is likely to cause abnormal cross-layer interactions, which may distort perceptions due to aberrant matching of top-down information with bottom-up information. If decelerated HFγ and subsequent cross-layer synchronization also underlie pathological psychosis, acceleration of HFγ could be the target for improved antipsychotic therapy.
Neuropsychopharmacology (2011) **36,** 519–528; doi:10.1038/npp.2010.183; published online 20 October 2010

Keywords: γ-oscillation; ketamine; phencyclidine; NMDA receptor; hallucinogenic; psychotomimetic

INTRODUCTION

Hallucinations are perceptions in the absence of a stimulus. Although hallucinations are often auditory in schizophrenia, hallucinations associated with neurodegenerative dementias such as Lewy body dementia and Parkinson's disease with dementia are normally visual (Metzler-Baddeley, 2007). Hallucinations and distortions of visual perception (Muetzelfeldt *et al*, 2008) are also a desired action of dissociative drugs, such as the *N*-methyl-D-aspartic acid (NMDA) receptor antagonists ketamine and phencyclidine (PCP). A single sub-anesthetic dose of ketamine or PCP is psychotomimetic (Farber, 2003) and as agents that enhance NMDA receptor function are antipsychotic (Kantrowitz *et al*, 2010; Schlumberger *et al*, 2010; Marek *et al*, 2010), NMDA receptor hypofunction is regarded as a shared process in both psychotic pathologies and substance abuse drugs (Coyle, 2006). Understanding the mechanism by which NMDA receptor hypofunction causes aberrant perceptions may lead to better antipsychotic treatment.

Perceptions may arise from matching of data-driven (bottom-up) information processing in the sensory cortices with (top-down) information driven by previous experiences stored in higher cortical areas. This process requires neuronal synchronization with millisecond precision provided by network oscillations at γ-frequencies (30–120 Hz) (Herrmann *et al*, 2004; Engel *et al*, 2001). Reduced NMDA receptor-mediated activation of interneurons in cortical networks leads to pyramidal neuron hyperexcitability (Homayoun and Moghaddam, 2007), which was hypothesized to cause aberrant perceptions by disruption of γ-synchronization (Marek *et al*, 2010). However, psychosis and hallucinations have rather been associated with γ-hypersynchronization (Hakami *et al*, 2009; Spencer *et al*, 2009; Flynn *et al*, 2008; Herrmann and Demiralp, 2005).

*Correspondence: Dr M Vreugdenhil, Neuronal Networks Group, School of Clinical and Experimental Medicine, University of Birmingham, Birmingham B15 2TT, United Kingdom, Tel: +44 121 4147629, Fax: +44 121 4147625, E-mail: m.vreugdenhil@bham.ac.uk
Received 8 July 2010; revised 7 September 2010; accepted 7 September 2010

In the neocortex, high-frequency γ-oscillations (HFγ; >70 Hz) coexist with low-frequency γ-oscillations (LFγ; <70 Hz) and the two can operate independently and serve different aspects of information processing (Wyart and Tallon-Baudry, 2008; Vidal *et al*, 2006; Crone *et al*, 2006). Recently, we demonstrated that HFγ and LFγ can coexist in the same column of the visual cortex *in vitro* and can operate independently (Oke *et al*, 2010). Interestingly, the NMDA receptor antagonist APV selectively reduced the dominant frequency of HFγ, so that it approached the frequency of the unaltered LFγ (Oke *et al*, 2010).

Therefore, we propose that NMDA receptor hypofunction causes phase coupling of two normally phase-independent γ-generating networks, causing hypersynchrony and a distortion of perception due to aberrant matching of top-down information with bottom-up information. In this study, we test the effect of NMDA receptor hypofunction on HFγ and LFγ recorded in the rat visual cortex *in vitro* and demonstrate that NMDA receptor hypofunction phase couples the two γ-generating networks.

MATERIALS AND METHODS

Preparation

Male adult Sprague Dawley rats (200–300 g, Charles-River, Margate, UK) were anesthetized by intraperitoneal injection of a ketamine (75 mg/kg)/medetomidine (1 mg/kg) mixture and killed by cardiac perfusion with a chilled sucrose-based solution containing 189 mM sucrose, 2.5 mM KCl, 26 mM $NaHCO_3$, 1.2 mM NaH_2PO_4, 0.1 mM $CaCl_2$, 5 mM $MgCl_2$, and 10 mM *D*-glucose; pH was set at 7.4. All procedures conformed to the UK Animals (Scientific Procedures) Act 1986. The brain was removed and coronal slices (400-μm thick) were cut around 7–6 mm caudal to bregma. The dorsal neocortex containing visual cortex areas V1 and V2 was isolated from the rest of the slice by scalpel cuts in chilled sucrose-based solution. Slices were either immediately placed at the interface between artificial cerebrospinal fluid (aCSF, at 7 ml/min) and moist carbogen (95% O_2 and 5% CO_2 at 300 ml/min) at 32°C, or stored in a static interface type chamber at 23°C for later use. aCSF contained 125 mM NaCl, 3 mM KCl, 26 mM $NaHCO_3$, 1.25 mM NaH_2PO_4, 2 mM $CaCl_2$, 1 mM $MgCl_2$, and 10 mM *D*-glucose; pH was set at 7.4. Slices were allowed to recover for 1 h before recordings started.

Electrophysiological Recordings

γ-Oscillations were evoked by adding kainate (400 nM) and the muscarinic acetylcholine receptor agonist carbachol (20 μM) (Buhl *et al*, 1998; Oke *et al*, 2010), and left to develop for 1 h before oscillation characteristics were further explored.

Field potentials were recorded using aCSF-filled glass pipette recording electrodes (4–5 MΩ), amplified with Neurolog NL104 AC-coupled amplifiers (Digitimer, Welwyn Garden City, UK), band-pass filtered at 1–200 Hz with Neurolog NL125 filters (Digitimer), and any noise locked to the mains supply (50 Hz) was removed using Humbug noise eliminators (Digitimer). The signal was then digitized and sampled at 2 kHz using a CED-1401 (Cambridge Electronic Design, Cambridge, UK) and Spike-2 software (Cambridge Electronic Design). Slices were scanned for sites where HFγ-oscillations and LFγ-oscillations were found in the same column, which was usually in the medial part of the secondary visual cortex.

Intracellular current-clamp recordings were made using sharp (60–80 MΩ) pipettes, filled with 3 M potassium methylsulfate. Using a MX1641 motorized microdrive (Siskyou, Grants Pass, OR, USA), the electrode was driven (at 5 μm steps) into the tissue parallel to the layers up to a depth of 250 μm in search for neurons. The membrane potential was amplified using an Axoclamp-2A amplifier (Axon Instruments, Burlingham, CA, USA), low-pass filtered at 2 kHz and sampled at 10 kHz. Impaled cells were first inspected and accepted for recording if the input resistance was >30 MΩ, the resting membrane potential was stable and more polarized than −55 mV in the presence of kainate and carbachol, and action potentials were overshooting.

Drugs were applied at ~2 h after application of kainate and carbachol when oscillation power and frequency were stable. Drug-induced changes after 25 min were compared with baseline values. Drugs were used diluted from the following frozen stock solutions. Ketamine; 50 mM in H_2O, PCP; 2 mM in H_2O (5S,10R)-(+)-5-methyl-10, 11-dihydro-5H-dibenzo[a,d]cyclohepten-5,10-imine maleate (MK-801); 10 mM in H_2O, $ZnCl_2$; 30 μM in H_2O, (aR,bS)-a-(4-Hydroxyphenyl)-b-methyl-4-(phenylmethyl)-1-piperidinepropanol maleate (Ro 25-6981); 10 mM in H_2O, (S)-3,5-dihydroxyphenylglycine (DHPG); 10 mM in H_2O. *D*-serine was directly added to aCSF. The *D*-serine-metabolizing enzyme *D*-amino acid oxidase (DAAO; 800 Units/ml) was derived from *Rhodotorula gracilis* and kindly donated by Professor Dale (University of Warwick). Ketamine, Ro 25-6981, and MK-801 were purchased from Tocris (Bristol, UK). All other drugs and aCSF salts were purchased from Sigma (Poole, UK). Ketamine and PCP were washed out for 30 min, and if the drug effect was reversible, a second higher concentration of the same drug was applied.

Data Analysis

The oscillation power was calculated from 60-s recording epochs by fast Fourier transforms (1-Hz bin size, Hanning window), using Spike-2 software. The γ-frequency band was set at 20–80 Hz for recording at 32°C, taking into account the temperature dependence of γ-oscillations observed in the visual cortex (Oke *et al*, 2010). The dominant oscillation frequency was determined as the frequency of peak power in the power spectrum smoothed by a 5-point simple moving average. To take into account possible changes in dominant oscillation frequency, the power was averaged over −5 to 5 Hz of the dominant frequency. Waveform cross-correlograms were calculated over 60-s digitally high-pass filtered (FIR at 10 Hz) epochs.

To obtain membrane waveform averages, field potential recordings were band-pass filtered (with a phase-true FIR filter) from 10 to 200 Hz. The maximum amplitude for γ-cycles was determined for this signal, so that on average one cycle per second exceeded this value. γ-Cycles of medium (0.4–0.6 times the maximum) amplitude were

marked at their trough minimum, and waveform averages of γ-cycles (>300 cycles, time-zeroed at the sorted marks) were then calculated from the 10-Hz high-pass (FIR) filtered membrane potential.

To determine the relationship between different events, peri-event interval distributions (between −50 and 50 ms) were calculated from timings of different events, and a distribution deviating significantly from a uniform distribution was considered to indicate a relationship between the timing of the two events. To determine the phase relationship between oscillations in recordings from different layers, peri-event intervals were calculated using MATLAB software (The MathWorks, Natick, MA, USA). Simultaneous 100-s recordings were band-pass filtered (with a phase-true FIR filter) at ±5 Hz of the dominant frequency of LFγ (determined in layer V) and of HFγ (determined in layer III). A Hilbert transform provided a discrete time analytical signal that was converted to phase angles in radians. From the Hilbert peak times from both recordings, peri-event interval distributions were calculated.

Statistics

Data are expressed as means ± SEM, and *n* indicates the number of slices or cells tested. The effect of drugs was tested by unpaired comparison with matched controls, using a two-tailed Student's *t*-test with and α-level of 0.05. Deviation from a uniform distribution was determined with the Kolmogorov–Smirnov (K–S) *Z*-test with and α-level of 0.05.

RESULTS

HFγ-Oscillations Coexist With LFγ-Oscillations

We induced rhythmic field potential oscillations in cortex slices by bath application of kainate (400 nM) and carbachol (20 μM), which substitute for the glutamatergic and cholinergic inputs lost due to slicing (Oke *et al*, 2010; Buhl *et al*, 1998). Oscillations had substantial power in the γ-frequency range (example in Figure 1a*i* and b*i*), which was set at 20–80 Hz for recording at 32°C, taking into account the temperature dependence of γ-oscillations (Oke *et al*, 2010). After 1 h, the visual cortex in each slice was scanned along layer IV to select a cortical column with oscillatory activity with power peaks in both the LFγ-oscillation frequency band (20–45 Hz) and the HFγ-oscillation frequency band (46–80 Hz) range (Oke *et al*, 2010), which was usually found in area V2M (Supplementary Figure S1). Simultaneous field potential recordings were then made from layer III (0.5 mm from the pial surface) and from layer V (1.2 mm from the pial surface, Supplementary Figure S1) of the selected column. The oscillatory activity in layer III (example in Figure 1a*i*, gray trace) was invariably faster than that in layer V (example in Figure 1a*i*). The power spectrum of the recording from layer III peaked at frequencies in the HFγ range (Table 1, example in Figure 1b*i*, gray line), whereas the power spectrum of the recording from layer V peaked at frequencies in the LFγ range (Table 1, example in Figure 1b*i*, black line).

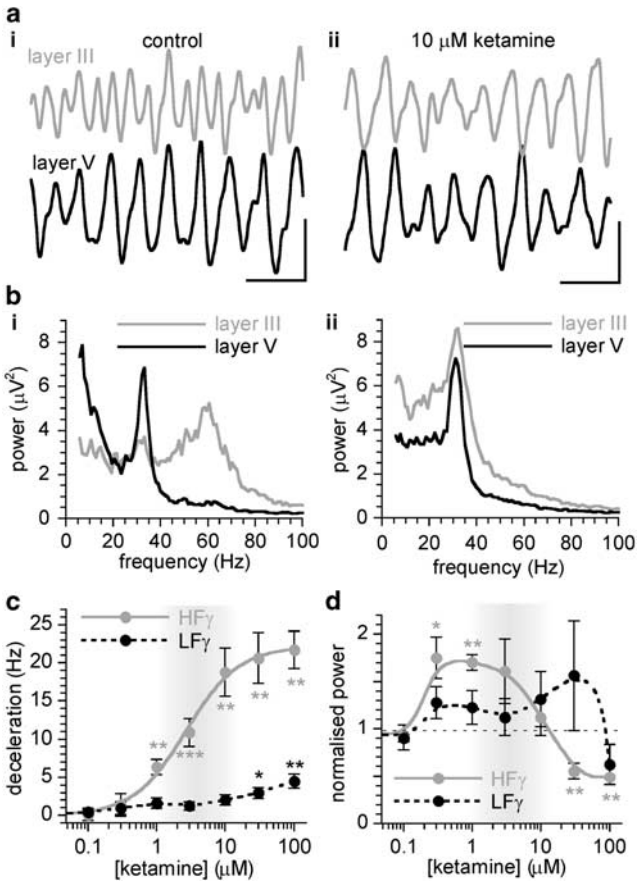

Figure 1 Ketamine decelerates HFγ selectively. (a) Example of oscillatory activity simultaneously recorded in layer III (gray line) and layer V (black line) of a cortical column in area V2M before (*i*) and 20 min after bath application of 10 μM ketamine (*ii*). Scale bars: 50 ms and 50 μV. (b) Power spectrum of 1-min recordings from layer III and layer V of the slice in (panel a) before (panel a*i*) and after ketamine (panel a*ii*). Ketamine reduces the frequency of HFγ in layer III, without affecting LFγ in layer V. (c) Concentration–effect relationship of the deceleration of the dominant oscillation frequency for HFγ in layer III (gray symbols) and LFγ in layer V (black symbols). Data are average and SEM of 3–8 observations per concentration. For each concentration, the ketamine-induced change in dominant frequency was compared with the change in control solution, with *indicating Student's *t*-test $P<0.05$; **$P<0.01$, and ***$P<0.001$. The deceleration as function of ketamine concentration is fitted with a sigmoid function for HFγ and with a smooth function for LFγ. Shaded area indicates concentrations reached with psycho-toxic ketamine doses in humans. (d) Dominant γ-power (average from −5 to +5 Hz from the dominant γ-oscillation frequency) normalized to control values as function of ketamine concentration for the same experiments as in panel c. Details as in panel c. Data are fitted with smooth functions.

Ketamine Selectively Decelerates HFγ

Application of the psychotomimetic drug ketamine (10 μM) reduced the dominant frequency of HFγ in layer III, without affecting the dominant frequency of LFγ in layer V (Table 1, example in Figure 1a*ii* and b*ii*). We determined the change in the dominant frequency of HFγ in layer III and of LFγ in layer V at 25 min after application of different ketamine concentrations and compared it with that after 25 min of continued perfusion with control aCSF (Table 1). Ketamine caused a significant reduction in dominant frequency of

Table 1 Pharmacological Modulation of HFγ and LFγ

Control values		LFγ in layer V		HFγ in layer III	
		γ-Power n (μV^2)	Frequency (Hz)	γ-Power n (μV^2)	Frequency (Hz)
		55 (26 ± 3)	34.3 ± 0.4	55 (33 ± 4)	54.1 ± 0.6
Changes		**n (%)**	**Δ (Hz)**	**n (%)**	**Δ (Hz)**
Control		8 (101 ± 6)	−0.5 ± 0.7	8 (95 ± 6)	−0.7 ± 1.0
Ketamine	10 μM	7 (131 ± 29)	−2.0 ± 0.8	7 (112 ± 19)	−18.8 ± 3.2**
PCP	1 μM	6 (99 ± 25)	−1.9 ± 0.9	6 (61 ± 12)*	−22.2 ± 2.8**
MK-801	10 μM	5 (163 ± 21)*	−1.4 ± 0.6	5 (127 ± 13)*	−18.2 ± 2.6**
DAAO	0.17 Units/ml	6 (112 ± 6)	0.4 ± 0.8	6 (71 ± 8)*	−10.4 ± 1.4**
Ro 25-6981	10 μM	4 (161 ± 18)**	−0.8 ± 0.5	4 (64 ± 9)**	−20.1 ± 2.2**
$ZnCl_2$	30 nM	5 (106 ± 3)	−1.1 ± 1.2	5 (114 ± 6)	−3.1 ± 1.2
NMDA	3 μM	5 (83 ± 6)*	0.6 ± 1.0	5 (73 ± 7)*	4.2 ± 0.6**
DHPG	10 μM	4 (81 ± 13)	1.1 ± 0.8	4 (129 ± 14)*	5.7 ± 1.6**
D-serine	100 μM	5 (93 ± 8)	−0.3 ± 0.7	5 (112 ± 7)	3.7 ± 0.7**

Recordings were made from layer III and layer V of slices with LFγ and HFγ. The drug-induced change of dominant γ-power (average over −5 to +5 Hz of the dominant frequency, expressed as % of pre-drug power), and the drug-induced shift in dominant frequency (in Hz) of LFγ in layer V and HFγ in layer III is given as mean ± SEM for n slices. Drug effects are compared with the change after 25 min in control solution. Statistical significant differences (unpaired Student's t-test) are indicated as $^*P<0.05$ and $^{**}P<0.01$.

HFγ at concentrations of 1 μM and above (Figure 1c). Ketamine-induced deceleration of HFγ in layer III, defined as ketamine-induced reduction in dominant frequency minus the change with control aCSF, as function of ketamine concentration (Figure 1c, gray symbols) was fitted with a sigmoid function of the form: effect = maximum effect/$(1+((\text{drug}/EC_{50})^{-h}))$, with a maximum effect of 22.1 ± 0.7 Hz, a concentration of half-maximum effect (EC_{50}) of 2.7 ± 0.3 μM, and a slope (h) of 1.1 ± 0.1. This EC_{50} is well within the range of concentrations obtained with sub-anesthetic doses used recreationally (shaded area in Figure 1c). Ketamine-induced deceleration of LFγ in layer V was only significant at very high concentrations (Figure 1c, black symbols). To allow for the frequency shift, the effect of ketamine on dominant γ-oscillation power was assessed by taking the average power over +5 and −5 Hz from the dominant frequency. The dominant HFγ power in layer III increased at lower concentrations and decreased at higher concentrations of ketamine (Figure 1d, gray symbols). The increase in dominant LFγ power in layer V at concentrations from 10 μM (Figure 1d, black symbols) may well reflect the contribution of decelerated HFγ in layer III. Effects of ketamine were completely reversible up to a concentration of 3 μM (not shown).

Deceleration of HFγ Causes Hypersynchrony

Under control conditions, HFγ in layer III was independent of LFγ in layer V (Oke *et al*, 2010). In the presence of ketamine, the difference between the dominant frequency of LFγ in layer V and that of decelerated HFγ in layer III became so small that there was a possibility that the two γ-oscillation-generating networks could become phase locked. We tested the prediction that ketamine would increase the phase link between the two oscillators, by determining the phase relationship between HFγ in layer III and LFγ in layer V from the peri-event intervals, calculated from a Hilbert transform of band-pass (±5 Hz around dominant frequency) filtered recordings. Before ketamine, the peri-event interval distribution was not different from uniform in 6 out of 7 slices (K–S test $P<0.05$, example in Figure 2a*i*), indicating the absence of a relationship between the phase of HFγ in layer III and the phase of LFγ in layer V. After ketamine (10 μM), the peaks in the inter-event distribution showed a significant relationship between the oscillation phase in layer III and that in layer V (example in Figure 2a*ii*). The K–S test Z increased from 1.11 ± 0.11 in controls to 4.23 ± 0.21 in ketamine (paired Student's t-test $P<0.001$, $n=7$, Figure 2a*iii*). On average, layer III γ-troughs were 4.3 ± 0.5 ms ahead of layer V γ-troughs. This indicates that, whereas in controls the two oscillators operate independently the ketamine-induced deceleration of HFγ in layer III causes phase coupling of the γ-generating networks in layers III and V.

Under control conditions, LFγ in layer V is spatially coherent, unlike HFγ in layer III (Oke *et al*, 2010). To test whether phase coupling of decelerated HFγ in layer III to LFγ would increase the spatial coherence of γ-oscillation in layer III, we determined the cross-correlation maximum between two electrodes placed 500 μm apart in layer III of the same slice. Cross-correlation was small in controls (example in Figure 2b*i*), but increased in the presence of ketamine (10 μM, example in Figure 2b*ii*). For five slices, the cross-correlation in layer III increased from 0.22 ± 0.02 in controls to 0.50 ± 0.05 in ketamine (paired Student's t-test

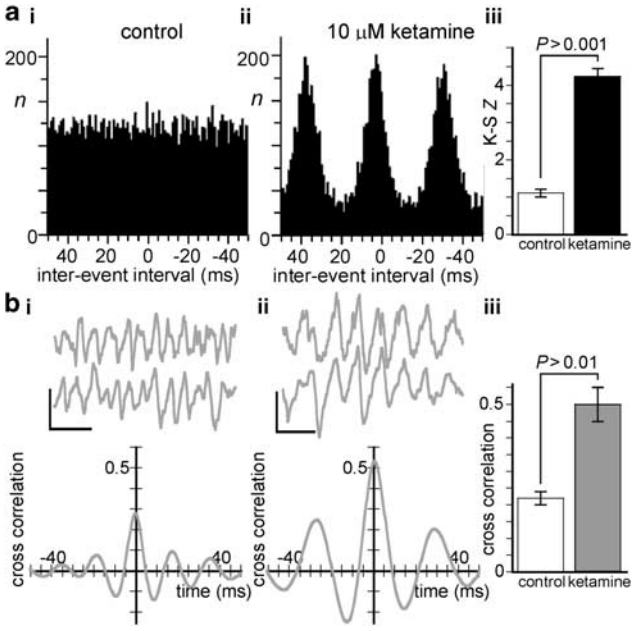

Figure 2 Ketamine increases phase coupling. (a) Peri-event interval distribution of the interval between phase peaks of the Hilbert transform of HFγ in layer III and those of LFγ in layer V before (*i*) and after 10 μM ketamine (*ii*) for the same slice as in Figure 1a/b. (*iii*) *Z*-value of the Kolmogorov–Smirnov test for uniform distribution for controls and ketamine. Data are mean ± SEM for $n = 7$. Ketamine phase locks the oscillation in layer III to the oscillation in layer V. (b) Simultaneous recordings from layer III at locations 500 μm apart (top panel) and waveform cross-correlogram (bottom panel) before (*i*) and after 10 μM ketamine (*ii*). (*iii*) Cross-correlation maximum in controls and ketamine. Data are mean ± SEM for $n = 5$. Ketamine increases maximum cross-correlation between layer III sites.

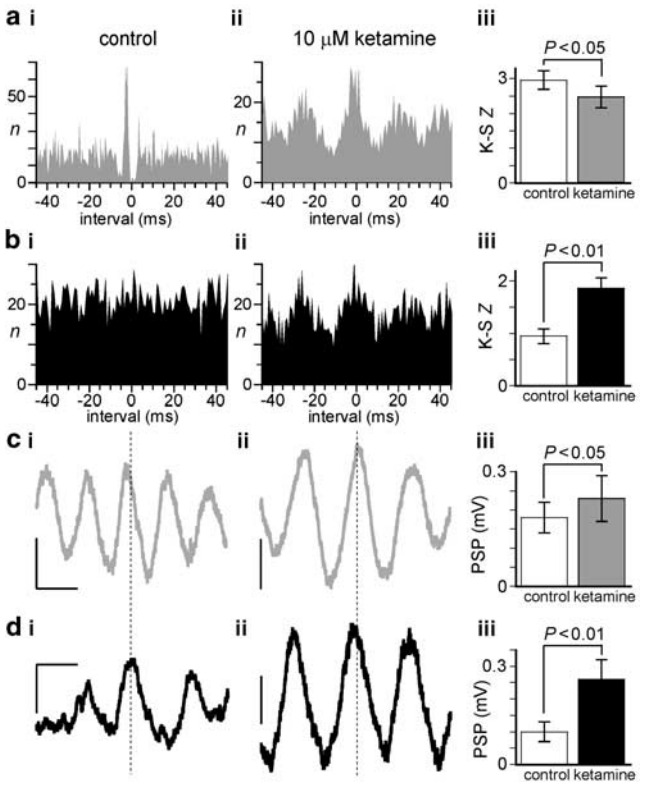

Figure 3 Ketamine effect on layer III pyramidal neurons. (a) Peri-event interval distribution of action potential peak times relative to HFγ troughs in layer III before (*i*) and after 10 μM ketamine (*ii*). (*iii*) *Z*-value of the Kolmogorov–Smirnov test for uniform distribution in controls and ketamine. Data are mean ± SEM for $n = 6$. (b) Same as in panel a, but relative to LFγ troughs in layer V. (c) Membrane potential (held just below firing threshold) waveform average time-zeroed to the HFγ troughs in layer III before (*i*) and after ketamine (*ii*). Scale bars: 20 μV, 20 ms. (*iii*) Maximum peak-to-trough amplitude of the postsynaptic potential (PSP) waveform average in controls and ketamine. Data give mean ± SEM for $n = 6$. (d) Same as in panel c, but time-zeroed to the LFγ troughs in layer V. Ketamine entrains layer III pyramidal neurons to LFγ troughs in layer V and increases LFγ-related rhythmic synaptic inputs.

$P < 0.01$, Figure 2b*iii*). For the same slices, the cross-correlation maximum between two electrodes placed 500 μm apart in layer V was not affected by ketamine (0.54 ± 0.05 in controls *vs* 0.58 ± 0.06 in ketamine, NS). This suggests that the increase in spatial coherence of γ-oscillations in layer III is due to phase coupling of decelerated HFγ in layer III to LFγ in layer V.

Ketamine Causes Entrainment of Layer III Pyramidal Neurons by LFγ

Like other cortical γ-oscillations (Buhl *et al*, 1998; Cunningham *et al*, 2003), HFγ in layer III is dependent on recurrent inhibition (Oke *et al*, 2010), and layer III pyramidal neuron firing is entrained by rhythmic IPSCs and EPSCs phase locked to HFγ in layer III (unpublished observations, MV). To test whether ketamine affects the relationship between the activity of layer III pyramidal neurons and γ-oscillations in different layers, we recorded cells in layer III under sharp electrode current-clamp conditions. Six cells identified as pyramidal neurons (see Supplementary Figure S2) were recorded before and after ketamine (10 μM).

To test the relationship between action potential firing times and γ-oscillation phase, neurons were made to fire at ~2 Hz by manually adjusting the holding current. The distribution of intervals between action potential peaks (500 per neuron) and HFγ troughs in layer III (example in Figure 3a*i*) was tested for uniformity. For 5 out of 6 neurons, the spike timing distribution showed a significant relationship (K–S test for uniformity, $P < 0.05$) between firing and HFγ troughs in layer III, with the peak firing probability in these neurons 4.3 ± 0.7 ms ahead of the HFγ trough. In contrast to the entrainment of firing by HFγ, the distribution of intervals between action potential peaks and LFγ troughs in layer V showed no entrainment of the same six-layer III pyramidal neurons by LFγ in layer V (example in Figure 3b*i*).

In the presence of ketamine (10 μM), the firing of the same layer III pyramidal neurons was still entrained by the now decelerated HFγ in layer III, but the relation was less tight (example in Figure 3a*ii*). The K–S test *Z* was reduced from 2.96 ± 0.26 in controls to 2.47 ± 0.31 in ketamine (paired Student's *t*-test $P < 0.05$, $n = 6$, Figure 3a*iii*). However, for 4 out of 6 layer III pyramidal neurons, the firing was now entrained by LFγ in layer V (example in Figure 3b*ii*), with the peak firing probability in these neurons 0.5 ± 1.0 ms after the HFγ trough. The K–S test

Z increased from 0.95 ± 0.14 in controls to 1.87 ± 0.19 in ketamine (paired Student's t-test $P<0.01$, $n=6$, Figure 3b*iii*). These observations demonstrate that layer III pyramidal neurons that under normal conditions ignore the LFγ in layer III become entrained by it in the presence of ketamine.

Ketamine Increases Rhythmic Synaptic Inputs

All pyramidal neurons recorded received a constant barrage of IPSPs and EPSPs. To determine how synaptic inputs are related to different γ-oscillations, we held the same neurons manually just below the firing threshold and constructed the membrane potential waveform averages, time-zeroed at the trough of medium-amplitude HFγ γ-cycles in layer III (example in Figure 3c*i*). The membrane potential γ-cycle had its peak amplitude 3.4 ± 0.6 ms ahead of the HFγ trough in layer III. The waveform averages of the membrane potential time-zeroed to the LFγ troughs in layer V (example in Figure 3d*i*) show that the membrane oscillation was only weakly coupled to LFγ in layer V, peaking 1.3 ± 0.8 ms ahead of the LFγ trough.

In the presence of ketamine, the membrane potential waveform average time zeroed at decelerated HFγ troughs in layer III was larger (example in Figure 3c*ii*) and peaked later (1.0 ± 0.7 ms, paired Student's t-test $P<0.01$, $n=6$). The maximum (peak-to-trough) amplitude was 0.23 ± 0.06 mV in ketamine *vs* 0.18 ± 0.04 mV in controls (paired Student's t-test $P<0.05$, $n=6$, Figure 3c*iii*). Ketamine strongly increased the maximum amplitude of the membrane potential waveform average for LFγ troughs in layer V (example in Figure 3d*ii*), without affecting the peak time (0.4 ± 0.7 ms after the LFγ trough, NS). The maximum amplitude was 0.26 ± 0.06 mV *vs* 0.10 ± 0.03 mV in controls (paired Student's t-test $P<0.01$, $n=6$, Figure 3d*iii*). These observations demonstrate that ketamine increases LFγ-related rhythmic synaptic inputs to layer III pyramidal neurons.

PCP Decelerates HFγ and Causes Hypersynchrony

The psychotomimetic drug PCP has a similar NMDA receptor-antagonistic action to ketamine, and we predicted that PCP would have a ketamine-like effect on γ-oscillations in the visual cortex. Like with ketamine, application of 1 μM PCP reversibly decelerated HFγ in layer III, but did not affect the dominant frequency of LFγ in layer V (Table 1, example in Supplementary Figure S3A/B). Like ketamine, 1 μM PCP phase locked the γ-generating networks in layers III and V that were independent in controls (Supplementary Figure S3C). The deceleration of HFγ in layer III as function of PCP concentration (Supplementary Figure S3D) was fitted with a sigmoid function with a maximum effect of 21.7 ± 0.9 Hz, an EC_{50} of 0.16 ± 0.02 μM, and a slope of 1.7 ± 0.3. PCP suppressed the dominant HFγ power at higher concentrations and increased the dominant LFγ power at intermediate concentrations (Supplementary Figure S3E), possibly due to contribution from decelerated HFγ in layer III. At concentrations obtained with doses used to induce hallucinations, PCP has the same network effects as ketamine.

NMDA Receptor-Modulating Drug Effects

Ketamine and PCP are not selective NMDA receptor antagonists and may exert their effect through inhibition of I_h (Tanabe, 2007) and/or dopamine D_2 receptor stimulation (Seeman *et al*, 2009). Therefore, we tested the effect of the selective non-competitive NMDA receptor antagonist MK-801. MK-801 (10 μM) decelerated HFγ, but left the dominant frequency of LFγ unchanged (Table 1). MK-801 increased the dominant γ-power of both HFγ and LFγ (Table 1). NMDA receptor activation also requires occupation of the glycine site by its endogenous ligand *D*-serine (Oliet and Mothet, 2009). We reduced endogenous *D*-serine levels by increasing *D*-serine metabolism by applying the enzyme DAAO. DAAO (0.17 Units/ml, 60 min) selectively decelerated HFγ (Table 1, example in Figure 4a). These observations, together with the increase in HFγ power observed with the competitive NMDA receptor antagonist APV (Oke *et al*, 2010), confirm that the HFγ-decelerating effect of ketamine and PCP is mediated through NMDA receptor antagonism.

To determine which NMDA receptor type is responsible, we tested the effect of Ro 25-6981 (10 μM), a selective antagonist of NR2B subunit-containing NMDA receptors (Fischer *et al*, 1997) and of nanomolar zinc, which selectively blocks NR2A subunit-containing NMDA receptors (Paoletti *et al*, 1997). Ro 25-6981 selectively decelerated HFγ, increased dominant LFγ power, and reduced dominant HFγ power (Table 1, example in Figure 4b). However, zinc (30 nM $ZnCl_2$) had no effect on the dominant frequency of HFγ or LFγ or on their dominant γ-power (Table 1). These observations indicate that the deceleration of HFγ by NMDA receptor antagonists is mediated by antagonism of NR2B subunit-containing NMDA receptors.

On the basis of the observation that NMDA receptor hypofunction can cause phase coupling of γ-oscillators by

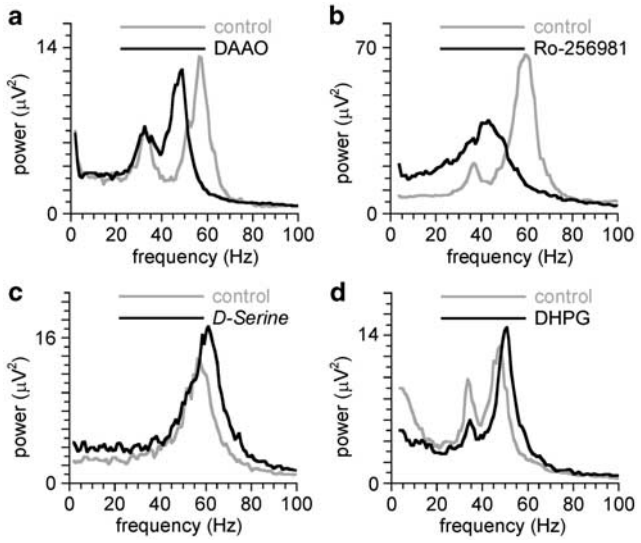

Figure 4 Effect of NMDA receptor modulation on HFγ. (a) Power spectrum of a 1-min recording from layer III before (gray line) and after reducing endogenous *D*-serine levels with DAAO (0.17 Units/ml, 60 min, black line). (b) Effect of the NR2B subunit-containing receptor antagonist Ro 25-6981 (10 μM, 25 min). Details as in panel a. (c) Effect of application of *D*-serine (100 μM). Details as in panel a. (d) Effect of facilitating NMDA receptor function by DHPG (10 μM). Details as in panel a.

selectively decelerating HFγ, we predicted that the opposite effect would be obtained by increasing NMDA receptor activation. To test this, we applied NMDA directly (Mann and Mody, 2010) to slices with HFγ and LFγ. NMDA (3 μM) selectively accelerated HFγ and suppressed the γ-power of both HFγ and LFγ (Table 1). NMDA receptor activity depends on activation of the glycine site of the receptor. Increasing glycine site occupation by applying a high concentration of *D*-serine (100 μM) selectively accelerated HFγ without affecting oscillation power (Table 1, example in Figure 4c). NMDA receptor activation can also be increased by activation of metabotropic glutamate group I receptors (Pisani *et al*, 1997). In line with this, the metabotropic glutamate group I receptor agonist DHPG (10 μM) selectively accelerated HFγ, without affecting the oscillation power (Table 1, example in Figure 4d). These observations confirm that, whatever the method, increasing NMDA receptor activity selectively accelerates HFγ.

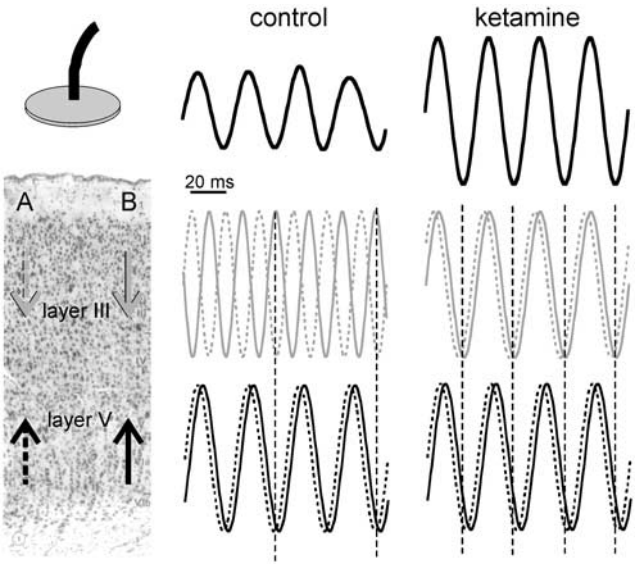

Figure 5 Illustration of the effect of hypersynchrony within and across layers. Recordings of γ-oscillations (modeled by sinusoids) from extracellular electrodes in two positions (500 μm apart, indicated in left panel) of layer III (gray traces) and layer V (bottom traces). In controls (left-hand traces), oscillations in layer III positions are not phase locked within the layer or with the oscillation in layer V. After ketamine (right-hand traces), the oscillation is phase locked within and between the layers, increasing the signal picked up from the surface (top traces: summation of sinusoids). Dotted lines indicate times at which potential firing times of layer III and layer V pyramidal neurons in position A would be nearly simultaneous, facilitating cross-layer interactions.

DISCUSSION

We investigated the effect of psychotomimetic NMDA receptor antagonists, ketamine and PCP, and demonstrated that in the visual cortex, NMDA receptor hypofunction causes phase coupling of both HFγ in layer III and layer III pyramidal neuron activity to LFγ in layer V, by selectively decelerating HFγ. This effect is mediated through *D*-serine-dependent NR2B subunit-containing receptors, and can be reversed by increasing NMDA receptor activity.

Ketamine and PCP selectively decelerate HFγ in layer III with an EC_{50} within the sub-anesthetic concentration range. At sub-anesthetic doses, ketamine strongly increases cortical LFγ power in the behaving rat (Hakami *et al*, 2009) and in healthy humans (Hong *et al*, 2010). This increase can be explained by the increase in HFγ power in layer III, and by the deceleration and increased spatial coherence of HFγ. Reducing the NMDA receptor-mediated drive of cortical interneurons increases pyramidal neuron firing rate (Homayoun and Moghaddam, 2007), which, according to computational modeling, would increase in cortical γ-power (Spencer, 2009). As the spatial coherence of HFγ is relatively low under control conditions (Oke *et al*, 2010), recordings taken from the cortical surface are likely to miss the HFγ that can be recorded with indwelling electrodes and magnetoencephalography (Tallon-Baudry, 2003). Deceleration of HFγ and subsequent phase coupling to the spatially more coherent LFγ will increase the spatial coherence of HFγ and the rhythmic IPSC amplitude in layer III pyramidal neurons, and hence, will increase the power of the oscillation recorded with surface electrodes (illustrated in Figure 5).

Why does NMDA receptor modulation selectively affect HFγ frequency? The relatively high frequency of HFγ could be caused by (1) faster IPSC decay kinetics (Whittington *et al*, 1995; Heistek *et al*, 2010), (2) smaller IPSC amplitude (Atallah and Scanziani (2009), but see Oke *et al* (2010)), (3) increased interneuron firing rate due to increased NMDA receptor-mediated depolarization and/or reduced tonic $GABA_A$ergic inhibition of interneurons (Mann and Mody, 2010), or (4) the selective NMDA receptor-mediated activation of fast-firing parvalbumin-expressing interneurons (Middleton *et al*, 2008). The consistent, bi-directional effects of modulating NMDA receptor activation on HFγ frequency suggest that NMDA receptor hypofunction decelerates HFγ by reduced activation of fast firing, probably parvalbumin-expressing interneurons in superficial layers that drive HFγ. Interneurons involved in LFγ in layer V may not be dependent on NMDA receptor-mediated activation. Indeed, $GABA_A$ergic IPSCs in layer V neurons are NMDA receptor activation independent (Ling and Benardo, 1995). As NMDA receptor-mediated modulation of interneuron activity can be presynaptic, NMDA receptor antagonists may selectively reduce glutamate release to interneurons involved in HFγ. Indeed, NR2B-containing (and not NR2A-containing) NMDA auto-receptors modulate glutamate release in the visual cortex and are located in layer II/III (Li *et al*, 2009). This is consistent with the differential effects of zinc and Ro 25-6981 in decelerating HFγ.

Psychosis and hallucinations have been associated with increased cortical LFγ (Flynn *et al*, 2008; Spencer *et al*, 2009; Becker *et al*, 2009), and gestalt-induced γ-oscillation is decelerated in the visual cortex of schizophrenics (Spencer *et al*, 2004). As NMDA receptor hypofunction is a common factor in the action of substance abuse drugs and schizophrenia-associated psychosis (Coyle, 2006; Farber, 2003), the latter could be due to an increased propensity of a cortical network to hypersynchronize (Spencer *et al*, 2009), due to network changes that can decelerate HFγ.

First, parvalbumin-expressing fast-firing interneurons may be functionally impaired. In the visual cortex of

schizophrenics, parvalbumin immunoreactivity is selectively reduced (Hashimoto *et al*, 2008). GABA synthesis is reduced in parvalbumin-expressing cortical interneurons (Hashimoto *et al*, 2003), possibly due to reduced activity of TrkB receptors, which are normally predominantly expressed on parvalbumin-expressing interneurons (Lewis *et al*, 2005), but are reduced in schizophrenics (Hashimoto *et al*, 2005). Increased activation of the remaining TrkB receptors may therefore have antipsychotic potential.

Second, NMDA receptor-dependent activation of interneurons may be reduced. Although the total cellular expression of NR2 proteins is not consistently altered in the cortex of schizophrenics, the trafficking of NR2B subunit-containing NMDA receptors to their presynaptic and postsynaptic locations is impaired (Kristiansen *et al*, 2010). In the chronic low-dose MK-801-treated rat model, parvalbumin-expressing interneurons have a reduced NMDA receptor expression (Xi *et al*, 2009). As increased activation of NR2B subunit-containing NMDA receptors accelerated HFγ, selective facilitation of these receptors may therefore have antipsychotic potential.

NMDA receptor activation requires co-activation of the glycine site by its endogenous ligand *D*-serine (Oliet and Mothet, 2009). Schizophrenia has been associated with aberrant NMDA receptor *D*-serine/glycine site function (Labrie and Roder, 2010), and increasing *D*-serine levels has an antipsychotic-like profile (Kantrowitz *et al*, 2010; Marek *et al*, 2010). Interestingly, in the rat visual cortex, glycine site agonists facilitate glutamate release in layer III by acting on presynaptic NR2B subunit-containing NMDA autoreceptors (Li *et al*, 2008). The deceleration of HFγ with reducing endogenous *D*-serine levels and the acceleration with exogenous *D*-serine confirm that the deceleration of HFγ is involved in the psychotic action of NMDA receptor hypofunction.

NMDA receptor activation is facilitated by metabotropic glutamate receptor group 1 activation (Pisani *et al*, 1997) through mGluR5 receptors. Although the mGluR5 expression is not altered in the cortex of schizophrenics (Gupta *et al*, 2005), increasing mGluR5 receptor activity has promising antipsychotic effects (Schlumberger *et al*, 2010), possibly due to the acceleration of HFγ observed with DHPG.

Third, non-NMDA receptor-dependent activation of fast-spiking interneurons may be impaired. Metabotropic glutamate receptor mGluR2-selective agonists selectively activate fast-spiking interneurons in the cortex (Sun *et al*, 2009) and have an antipsychotic action (Marek *et al*, 2010). The expression of kainate receptor subunit GluR5 (not GluR6) mRNA was reduced in cortical interneurons of schizophrenics (Woo *et al*, 2007). As the GluR5 subunit-selective kainate receptor agonist ATPA accelerated HFγ frequency (Oke *et al*, 2010), selective GluR5 potentiators may have an antipsychotic potential (Marek *et al*, 2010).

At a cellular level, the ketamine-induced deceleration of HFγ caused the firing of layer III pyramidal neurons to be entrained by LFγ in layer V. Whereas under control conditions, the firing of pyramidal neurons in superficial layers is independent of those in the deep layers, NMDA receptor hypofunction aligns the firing of the two populations, increasing the interactions between the layers (illustrated in Figure 5). As the decelerated HFγ in layer III phase leads LFγ in layer V, as in the somatosensory cortex under control conditions (Buhl *et al*, 1998), EPSPs from layer III pyramidal neurons may arrive just before IPSCs in layer V pyramidal neurons. This is likely to increase the information transfer between the layers during γ-oscillations. In addition, it may increase the synaptic strength of layer III to layer V pyramidal neuron connections through Hebbian plasticity and change information transfer long term. In addition, phase coupling of neuronal firing across layers is likely to increase burst firing in layer V pyramidal neurons that stretch through all layers (Larkum *et al*, 1999, 2004).

Functionally, it is tempting to speculate how hallucinations can arise from the increased coupling of processes in superficial layers and deep layers. Coexistence of HFγ and LFγ is found throughout the cortex, including the auditory cortex and prefrontal cortex (Crone *et al*, 2006). In the visual cortex, HFγ and LFγ are associated with different aspects of visual information processing (Wyart and Tallon-Baudry, 2008; Vidal *et al*, 2006; Chaumon *et al*, 2009) and relate to the degree of top-down or bottom-up processing (Tallon-Baudry, personal communication). Conscious perception of complex visual stimuli may need the matching of stimulus-driven bottom-up information with memory-based top-down predictions (Wyart and Tallon-Baudry, 2008; Herrmann *et al*, 2004; Engel *et al*, 2001). Top-down processes may modulate the temporal structure of bottom-up processes (Engel *et al*, 2001), and/or boost the response of layer V neurons when bottom-up and top-down information arrives simultaneously at basal and apical dendrites, respectively (Siegel and Konig, 2003; Larkum *et al*, 2004). Therefore, the phase coupling induced by NMDA receptor hypofunction may cause erroneous matching and hence distortion of perception of bottom-up information, or even perception without it during hallucinations. *In vivo* experiments are required to test the relationship between increased phase coupling of HFγ and LFγ and psychosis.

The negative symptoms in schizophrenics are associated with γ-band hyposynchronization (Spencer *et al*, 2009; Herrmann and Demiralp, 2005), which poses the question, how can γ-band hypersynchronization arise from the same distorted network? Computational modeling has demonstrated that different kinds of network abnormalities associated with schizophrenia can produce γ-oscillation deficits and increases (Spencer, 2009). We propose that even in a network with reduced LFγ, the coincidence of several of the modulatory factors that can each cause selective deceleration of HFγ in superficial layers, may cause a temporary cross-layer γ-band hypersynchronization and consequent distortion of perception, due to aberrant matching of top-down information with bottom-up information. Our study suggests that a combination of therapies to counteract several of these modulating factors may provide the most effective antipsychotic therapy.

ACKNOWLEDGEMENTS

We thank the Medical Research Council (UK) for support. We also thank Professor Jefferys (University of Birmingham) for discussion and use of equipment, as well as

B Shakila and Professor Dale (University of Warwick) for the production and kind donation of DOOA.

DISCLOSURE

The authors declare that, except for income received from the primary employer, or stipends unrelated to pharmaceutical corporations, no financial support or compensation has been received from any individual or corporation over the last 3 years of research and that there are no personal financial holdings that could be perceived as constituting a potential conflict of interest.

REFERENCES

Atallah BV, Scanziani M (2009). Instantaneous modulation of gamma oscillation frequency by balancing excitation with inhibition. *Neuron* **62**: 566–577.

Becker C, Gramann K, Muller HJ, Elliott MA (2009). Electrophysiological correlates of flicker-induced color hallucinations. *Conscious Cogn* **18**: 266–276.

Buhl EH, Tamas G, Fisahn A (1998). Cholinergic activation and tonic excitation induce persistent gamma oscillations in mouse somatosensory cortex *in vitro*. *J Physiol (Lond)* **513**: 117–126.

Chaumon M, Schwartz D, Tallon-Baudry C (2009). Unconscious learning versus visual perception: dissociable roles for gamma oscillations revealed in MEG. *J Cogn Neurosci* **21**: 2287–2299.

Coyle JT (2006). Substance use disorders and schizophrenia: a question of shared glutamatergic mechanisms. *Neurotox Res* **10**: 221–233.

Crone NE, Sinai A, Korzeniewska A (2006). High-frequency gamma oscillations and human brain mapping with electrocorticography. *Prog Brain Res* **159**: 275–295.

Cunningham MO, Davies CH, Buhl EH, Kopell N, Whittington MA (2003). Gamma oscillations induced by kainate receptor activation in the entorhinal cortex *in vitro*. *J Neurosci* **23**: 9761–9769.

Engel AK, Fries P, Singer W (2001). Dynamic predictions: oscillations and synchrony in top-down processing. *Nat Rev Neurosci* **2**: 704–716.

Farber NB (2003). The NMDA receptor hypofunction model of psychosis. *Ann N Y Acad Sci* **1003**: 119–130.

Fischer G, Mutel V, Trube G, Malherbe P, Kew JN, Mohacsi E *et al.* (1997). Ro 25-6981, a highly potent and selective blocker of N-methyl-D-aspartate receptors containing the NR2B subunit. Characterization *in vitro*. *J Pharmacol Exp Ther* **283**: 1285–1292.

Flynn G, Alexander D, Harris A, Whitford T, Wong W, Galletly C *et al.* (2008). Increased absolute magnitude of gamma synchrony in first-episode psychosis. *Schizophr Res* **105**: 262–271.

Gupta DS, McCullumsmith RE, Beneyto M, Haroutunian V, Davis KL, Meador-Woodruff JH (2005). Metabotropic glutamate receptor protein expression in the prefrontal cortex and striatum in schizophrenia. *Synapse* **57**: 123–131.

Hakami T, Jones NC, Tolmacheva EA, Gaudias J, Chaumont J, Salzberg M *et al.* (2009). NMDA receptor hypofunction leads to generalized and persistent aberrant gamma oscillations independent of hyperlocomotion and the state of consciousness. *PLoS One* **4**: e6755.

Hashimoto T, Bazmi HH, Mirnics K, Wu Q, Sampson AR, Lewis DA (2008). Conserved regional patterns of GABA-related transcript expression in the neocortex of subjects with schizophrenia. *Am J Psychiatry* **165**: 479–489.

Hashimoto T, Bergen SE, Nguyen QL, Xu B, Monteggia LM, Pierri JN *et al.* (2005). Relationship of brain-derived neurotrophic factor and its receptor TrkB to altered inhibitory prefrontal circuitry in schizophrenia. *J Neurosci* **25**: 372–383.

Hashimoto T, Volk DW, Eggan SM, Mirnics K, Pierri JN, Sun Z *et al.* (2003). Gene expression deficits in a subclass of GABA neurons in the prefrontal cortex of subjects with schizophrenia. *J Neurosci* **23**: 6315–6326.

Heistek TS, Timmerman AJ, Spijker S, Brussaard AB, Mansvelder HD (2010). GABAergic synapse properties may explain genetic variation in hippocampal network oscillations in mice. *Front Cell Neurosci* **4**: 18-doi:10.3389/fncel.2010.00018.

Herrmann CS, Demiralp T (2005). Human EEG gamma oscillations in neuropsychiatric disorders. *Clin Neurophysiol* **116**: 2719–2733.

Herrmann CS, Munk MH, Engel AK (2004). Cognitive functions of gamma-band activity: memory match and utilization. *Trends Cogn Sci* **8**: 347–355.

Homayoun H, Moghaddam B (2007). NMDA receptor hypofunction produces opposite effects on prefrontal cortex interneurons and pyramidal neurons. *J Neurosci* **27**: 11496–11500.

Hong LE, Summerfelt A, Buchanan RW, O'Donnell P, Thaker GK, Weiler MA *et al.* (2010). Gamma and delta neural oscillations and association with clinical symptoms under subanesthetic ketamine. *Neuropsychopharmacology* **35**: 632–640.

Kantrowitz JT, Malhotra AK, Cornblatt B, Silipo G, Balla A, Suckow RF *et al.* (2010). High dose D-serine in the treatment of schizophrenia. *Schizophr Res* **121**: 125–130.

Kristiansen LV, Bakir B, Haroutunian V, Meador-Woodruff JH (2010). Expression of the NR2B-NMDA receptor trafficking complex in prefrontal cortex from a group of elderly patients with schizophrenia. *Schizophr Res* **119**: 198–209.

Labrie V, Roder JC (2010). The involvement of the NMDA receptor D-serine/glycine site in the pathophysiology and treatment of schizophrenia. *Neurosci Biobehav Rev* **34**: 351–372.

Larkum ME, Senn W, Luscher HR (2004). Top-down dendritic input increases the gain of layer 5 pyramidal neurons. *Cereb Cortex* **14**: 1059–1070.

Larkum ME, Zhu JJ, Sakmann B (1999). A new cellular mechanism for coupling inputs arriving at different cortical layers. *Nature* **398**: 338–341.

Lewis DA, Hashimoto T, Volk DW (2005). Cortical inhibitory neurons and schizophrenia. *Nat Rev Neurosci* **6**: 312–324.

Li YH, Han TZ, Meng K (2008). Tonic facilitation of glutamate release by glycine binding sites on presynaptic NR2B-containing NMDA autoreceptors in the rat visual cortex. *Neurosci Lett* **432**: 212–216.

Li YH, Wang J, Zhang G (2009). Presynaptic NR2B-containing NMDA autoreceptors mediate gluta-matergic synaptic transmission in the rat visual cortex. *Curr Neurovasc Res* **6**: 104–109.

Ling DS, Benardo LS (1995). Recruitment of GABAA inhibition in rat neocortex is limited and not NMDA dependent. *J Neurophysiol* **74**: 2329–2335.

Mann EO, Mody I (2010). Control of hippocampal gamma oscillation frequency by tonic inhibition and excitation of interneurons. *Nat Neurosci* **13**: 205–212.

Marek GJ, Behl B, Bespalov AY, Gross G, Lee Y, Schoemaker H (2010). Glutamatergic (N-methyl-D-aspartate receptor) hypofrontality in schizophrenia: too little juice or a miswired brain? *Mol Pharmacol* **77**: 317–326.

Metzler-Baddeley C (2007). A review of cognitive impairments in dementia with Lewy bodies relative to Alzheimer's disease and Parkinson's disease with dementia. *Cortex* **43**: 583–600.

Middleton S, Jalics J, Kispersky T, LeBeau FE, Roopun AK, Kopell NJ *et al.* (2008). NMDA receptor-dependent switching between different gamma rhythm-generating microcircuits in entorhinal cortex. *Proc Natl Acad Sci USA* **105**: 18572–18577.

Muetzelfeldt L, Kamboj SK, Rees H, Taylor J, Morgan CJ, Curran HV (2008). Journey through the K-hole: phenomenological aspects of ketamine use. *Drug Alcohol Depend* **95**: 219–229.

Oke OO, Magony A, Anver H, Ward PD, Jiruska P, Jefferys JGR *et al.* (2010). High-frequency gamma oscillations coexist with

low-frequency gamma oscillations in the rat visual cortex *in vitro*. *Eur J Neurosci* **31**: 1435–1445.

Oliet SH, Mothet JP (2009). Regulation of N-methyl-D-aspartate receptors by astrocytic D-serine. *Neuroscience* **158**: 275–283.

Paoletti P, Ascher P, Neyton J (1997). High-affinity zinc inhibition of NMDA NR1-NR2A receptors. *J Neurosci* **17**: 5711–5725.

Pisani A, Calabresi P, Centonze D, Bernardi G (1997). Enhancement of NMDA responses by group I metabotropic glutamate receptor activation in striatal neurones. *Br J Pharmacol* **120**: 1007–1014.

Schlumberger C, Pietraszek M, Gravius A, Danysz W (2010). Effects of a positive allosteric modulator of mGluR5 ADX47273 on conditioned avoidance response and PCP-induced hyperlocomotion in the rat as models for schizophrenia. *Pharmacol Biochem Behav* **95**: 23–30.

Seeman P, Guan HC, Hirbec H (2009). Dopamine D2High receptors stimulated by phencyclidines, lysergic acid diethylamide, salvinorin A, and modafinil. *Synapse* **63**: 698–704.

Siegel M, Konig P (2003). A functional gamma-band defined by stimulus-dependent synchronization in area 18 of awake behaving cats. *J Neurosci* **23**: 4251–4260.

Spencer KM (2009). The functional consequences of cortical circuit abnormalities on gamma oscillations in schizophrenia: insights from computational modeling. *Front Hum Neurosci* **3**: 33.

Spencer KM, Nestor PG, Perlmutter R, Niznikiewicz MA, Klump MC, Frumin M *et al.* (2004). Neural synchrony indexes disordered perception and cognition in schizophrenia. *Proc Natl Acad Sci USA* **101**: 17288–17293.

Spencer KM, Niznikiewicz MA, Nestor PG, Shenton ME, McCarley RW (2009). Left auditory cortex gamma synchronization and auditory hallucination symptoms in schizophrenia. *BMC Neurosci* **10**: 85: doi:10.1186/1471-2202-10-85.

Sun QQ, Zhang Z, Jiao Y, Zhang C, Szabo G, Erdelyi F (2009). Differential metabotropic glutamate receptor expression and modulation in two neocortical inhibitory networks. *J Neurophysiol* **101**: 2679–2692.

Tallon-Baudry C (2003). Oscillatory synchrony and human visual cognition. *J Physiol (Paris)* **97**: 355–363.

Tanabe M (2007). Inhibition of hyperpolarization-activated cation currents by phencyclidine and some sigma ligands in rat hippocampal CA1 pyramidal neurons *in vitro*. *Neuropharmacology* **53**: 406–414.

Vidal JR, Chaumon M, O'Regan JK, Tallon-Baudry C (2006). Visual grouping and the focusing of attention induce gamma-band oscillations at different frequencies in human magnetoencephalogram signals. *J Cogn Neurosci* **18**: 1850–1862.

Whittington MA, Traub RD, Jefferys JGR (1995). Synchronized oscillations in interneuron networks driven by metabotropic glutamate receptor activation. *Nature* **373**: 612–615.

Woo TU, Shrestha K, Amstrong C, Minns MM, Walsh JP, Benes FM (2007). Differential alterations of kainate receptor subunits in inhibitory interneurons in the anterior cingulate cortex in schizophrenia and bipolar disorder. *Schizophr Res* **96**: 46–61.

Wyart V, Tallon-Baudry C (2008). Neural dissociation between visual awareness and spatial attention. *J Neurosci* **28**: 2667–2679.

Xi D, Zhang W, Wang HX, Stradtman GG, Gao WJ (2009). Dizocilpine (MK-801) induces distinct changes of N-methyl-D-aspartic acid receptor subunits in parvalbumin-containing interneurons in young adult rat prefrontal cortex. *Int J Neuropsychopharmacol* **12**: 1395–1408.

Supplementary Information accompanies the paper on the Neuropsychopharmacology website (http://www.nature.com/npp)